Journal of Engineering Science and Technology
Vol. 11, No. 3 (2016) 346 - 361

THERMAL DRIFT CHARACTERISTICS OF CAPACITIVE PRESSURE SENSORS

ABDELAZIZ BEDDIAF[1,2,*], FOUAD KERROUR[2], SALAH KEMOUCHE[2]

[1] University of Khenchela, Khenchela, Algeria
[2] MoDERNa Laboratory, University of Constantine 1, Route d' Ain El Bey, 25000 Constantine, Algeria
*Corresponding Author: beddiafaziz@yahoo.fr

Abstract

The capacitive pressure sensors based on silicon are characterized by their very high sensitivities and their low power consumption. Nevertheless, their thermal behavior remains more or less unpredictable because they can indicate very high thermal coefficients. The study of the thermal behavior of these sensors is essential to define the parameters that cause the output characteristics drift. In this study, we modeled the thermal behavior of this sensors, using Finite Element Analysis (*FEA*) made in COMSOL. The model solved by COMSOL environment takes into account the entire sensor and thermal effects due to the temperature considering the materials' properties, the geometric shape and also the heat transfer mechanisms. By COMSOL we determine how the temperature affects the sensor during the manufacturing process. For that end, we calculated the thermal drift of capacitance at rest, the thermal coefficients and we compared them with experimental results to validate our model. Further, we studied the thermal drift of sensor characteristics both at rest and under constant and uniform pressure. Further, our study put emphasis on the geometric influence parameters on these characteristics to optimize the sensor performance. Finally, this study allows us to predict the sensor behavior against temperature and to minimize this effect by optimizing the geometrical parameters.

Keywords: Temperature coefficient, Capacitive pressure sensor, Silicon, COMSOL.

1. Introduction

Fields require the application of pressure sensors with increasingly high performances [1-15]. The capacitive pressure sensor, in which the capacitance of a chamber changes with application of pressure, finds extensive applications because of its low power consumption and high sensitivity [3, 8]. The type of sensors will generate an electrical signal as a result of the elastic deformation of the membrane,

Nomenclatures

A	Area of fixed plate, m^2
ab	Bond width, m
C	Capacitance, F
C_0	Capacitance at rest, F
d	Distance between the two plates, m
D	Coefficient of rigidity
E	Young moduls, Pa
G	Coulomb modulus, Pa
hp	Substrate thickness, m
hs	Membrane thickness, m
P	Applied pressure, Pa
R	Radius of the diaphragm, m
R_e	Radius of the fixed electrode, m
S	Sensor sensitivity, F/Pa
T_C	Temperature coefficient, ppm/°C
ν	Poisson ratio
w	Membrane deflection, m
w_o	Central maximum deflection, m
w_{py}	Displacement of fixed plate, m
w_{Si}	Displacement of movable plate, m

Greek Symbols

ε_r	Air relative permittivity
ε_o	Vacuum permittivity, F/m

Abbreviations

FEA	Finite Element Analysis

as in the case of other sensors, such as piezoresistive types. The study of the thermal behavior of these sensors is essential to define the parameters that cause the output characteristics drift. A. Boukabache introduced a theoretical approach and experiments to analyse the electrical response of a piezoresistive pressure sensor fabricated using monocrystalline Silicon. His analysis focuses on the thermal behavior of the offset voltage and its origins [16]. The temperature effects and the compensation for temperature drift of offset voltage in silicon piezoresistive pressure sensor was indicated by U. Aljancic [15]. In a previous study [17] we have analysed the effect of temperature and doping level on the characteristics of this sensor type. More recently, in another work, we made a thermomechanical modeling of a piezoresistive pressure sensor [18]. The thermal behavior of capacitive pressure sensors fabricated using silicon and Pyrex wafers was presented by G. Blasquez [13].

This paper seeks to study the thermal drift of sensor characteristics at rest and under constant and uniform pressure. Besides, the study aims to explore the geometric influence parameters on these characteristics to optimize the sensor performance, using Finite Element Analysis (*FEA*) made in COMSOL. The model solved by COMSOL environment takes into account the entire sensor and thermal effects caused by the manufacturing process of the device. This allows better understanding and quantifying the thermal drifts that can affect the sensor.

2. Methodology and Theory

2.1. Membrane deflection

Based on the assumption of thin elastic anisotropic membrane under small deflection, the deflection of a circular diaphragm Fig. 1 with fully clamped perimeter as a function of radius, *w(r)*, is given by the following Lagrange equation [19-20]:

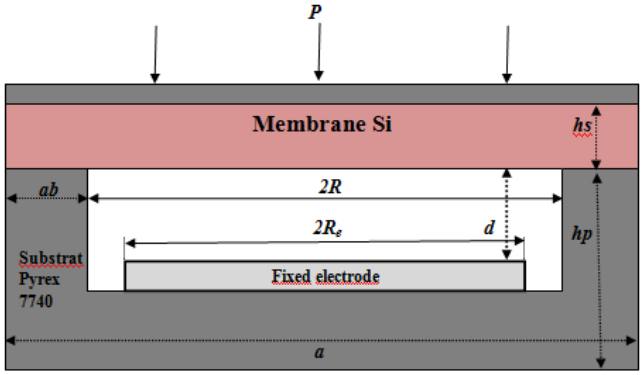

Fig. 1. Capacitive pressure sensor structure.

$$\nabla^4 w(r) = \frac{1}{r}\frac{\partial}{\partial r}\left[r\frac{\partial}{\partial r}\left[r\frac{\partial}{\partial r}\left(r\frac{\partial w(r)}{\partial r}\right)\right]\right] = \frac{P}{D} \tag{1}$$

where r is the distance from the center of the diaphragm, D is the flexural rigidity and P is the uniform applied pressure [21]:

$$D = \frac{E\,h^3}{12\,(1-\nu^2)} \tag{2}$$

where ν is the Poisson's ratio and E is the Young module. The boundary conditions imposed by the membrane embedding on its edges [21] are:

$$w\,(r=R)=0\,,\ \left.\frac{\partial w}{\partial r}\right|_{(r=R)} = 0 \tag{3}$$

The analytical solution of Eq. (1) can be adopted in the case of small deflection of the diaphragm, compared with thickness of the diaphragm [14, 20]:

$$w(r) = \frac{P\,(R^2-r^2)^2}{64\,D} = w_0\left[1-\left(\frac{r}{R}\right)^2\right]^2 \tag{4}$$

where R is the radius of the plate and w_0 is the central maximum deflection given by:

$$w_0 = \frac{P\,A^2}{\pi^2 64\,D} \tag{5}$$

2.2. Capacitive pressure modeling

Figure 1 shows the principle scheme of a capacitive pressure sensor. The thin silicon membrane constitutes the movable plate of the parallel-plate capacitor. A metallic layer deposited on the Pyrex 7740 substrate constitutes the fixed plate of the capacitor. The two plates, fabricated separately, have been bonded anodically by the electrostatic seal technique. The deformation change is due to the applied pressure *P* which, in turn, changes the capacitance *C(P)*. The capacitance value at rest is given by [11]:

$$C_0 = \frac{\varepsilon_0 \varepsilon_r A}{d} \tag{6}$$

where A is the area of fixed plate, $\boldsymbol{d}$ the distance between the two plates, $\boldsymbol{\varepsilon_0}$ is the vacuum permittivity, ε_r is the air relative permittivity and R *is* the radius of the diaphragm. At equilibrium the capacitance is expressed by [11]:

$$C(P) = \iint_A \frac{\varepsilon_0 \varepsilon_r}{d - w(r)} dA \tag{7}$$

We replace *w(r)* in Eq. (8) using Eq. (4), we obtain the expression given by [8]:

$$C(P) = C_0 \left[1 + \frac{1}{3}\left(\frac{w_0}{d}\right) + 0.2\left(\frac{w_0}{d}\right)^2 \right] \tag{8}$$

2.3. Temperature coefficient

According to Fig. 1, which shows the simple capacitive pressure sensor, the temperature T can modify diaphragm thickness *hs,* the distance between the two plates *d,* the bond width *ab* and as a consequence C. In other words, C is also a function of T. The thermal behavior of C is usually characterized by the parameter T_C that is called the temperature coefficient. In an extended temperature range, T_C is a function of T. Therefore, the most appropriate definition of T_C is the relative partial derivative of C [13]:

$$T_C\left[C(T)\right] = \frac{1}{C(T)} \frac{\partial C(T)}{\partial T} \tag{9}$$

3. Finite Element Simulation

The material property of Silicon and pyrex7740 used in simulation are listed in Table 1.

Table 1. Material property of silicon and pyrex 7740.

Layer	Silicon [11, 19]	Pyrex 7740 [11, 19]
Young's Modulus (GPa)	130	60
Poisson's Ratio	0.28	0.25
Thermal expansion coefficient (ppm/°C)	2.33	3.25
Density (g/cm³)	2.33	2.23

3.1. Finite element model validation

To validate the finite element model developed in COMSOL we compared some results obtained by the model with results obtained experimentally. In Fig. 2 the capacitive simulated response as a function of the pressure is identical with that found experimentally [11]. However, according to the capacitive response and the temperature coefficient simulated at rest in the curves of Figs. 3 and 4, there is a slight difference in the values of the elevated results caused by the manufacturing process of the device. The comparison of the obtained results allows us to validate the simulation model in COMSOL Multiphisycs environment.

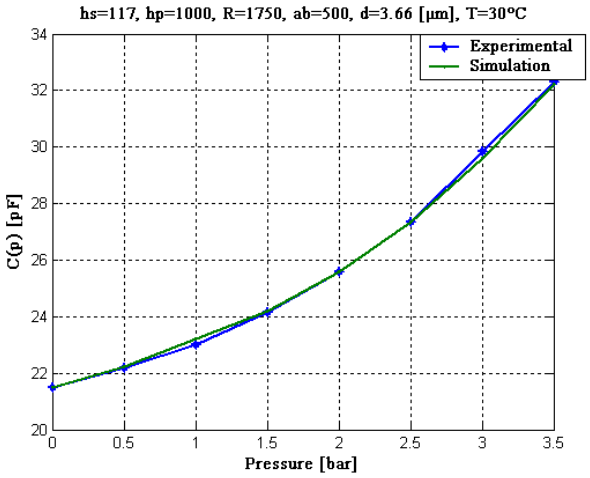

Fig. 2. Capacitance variation vs. applied pressure.

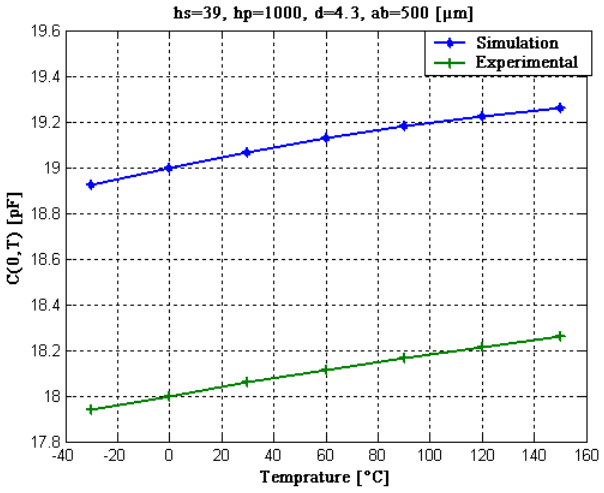

Fig. 3. Capacitance thermal variations.

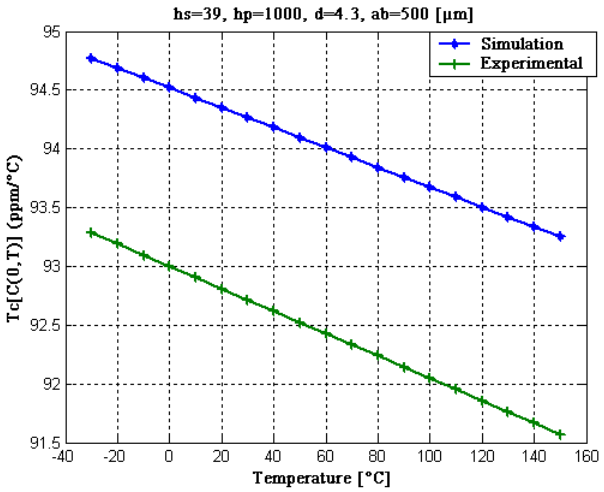

Fig. 4. Temperature coefficient.

3.2. Thermal study

In this section the sensor thermal behavior study at rest *(P = 0)* has been performed. For this, we adopt the model of Finite Element Analysis in COMSOL. The thermal drifts of capacitive pressure sensors are mainly due to thermo-mechanical strain caused by the difference in coefficient of thermal expansion of Silicon and Pyrex. However, the electrical and mechanical properties of these materials have an impact, but, because we did not have enough information on the impact of these properties on the thermal behavior of the sensor, we focused on the thermal drift study. Further details of the *FEA* thermo-mechanical modeling process can be found in a former study [18]. We will study the thermal drift of capacitive pressure sensor characteristics at rest as we will study, the geometric influence parameters on these characteristics to optimize the sensor performance. The choice of these geometrical parameters for simulations is taken from previous work [11].

The capacitive pressure sensors structure composed of a thin silicon membrane with a thermal expansion coefficient similar to that of Pyrex glass 7740 is used for anodic bonding to minimize thermo mechanical stress [12, 13].

3.2.1. Membrane thickness effect *hs*

Figure 5 shows the variations in capacitance at rest as a function of temperature in the range of -30 ° C to 150 ° C for different *hs*. In this case, we consider that the sensor is a fully deformable structure $w=w_{Py}- w_{Si}$, where w_{Py} and w_{Si} represent, respectively, the displacement of movable and fixed plate [22]. In the low temperature, as the deflection *w* changes in the negative sense [22], it causes a decrease of the capacitor *C(0,T)* by decreasing the *hs*. However, when $T > 0$ the deflection *w* changes in the positive sense [22], the *C(0,T)* is inversely proportional to *hs*. Nevertheless, these variations have much smaller amplitude and exhibit a quasi-linear behavior.

It can be seen in Fig. 6 that the temperature coefficients are a highly decreasing function of the membrane thickness *hs*.

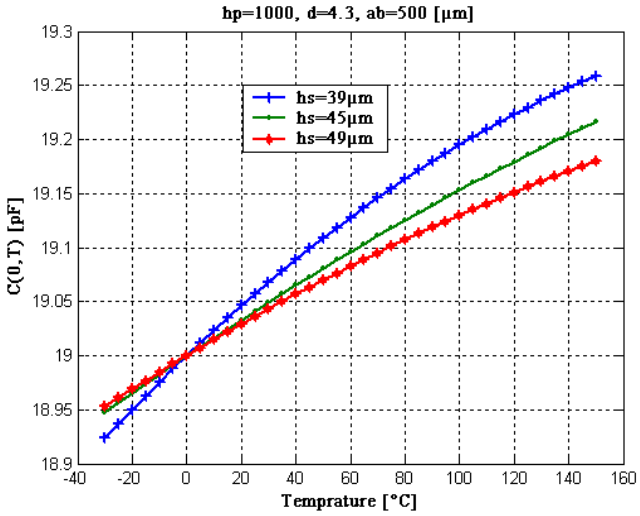

Fig. 5. Variation of the capacitance at rest as function of the temperature for different *hs*.

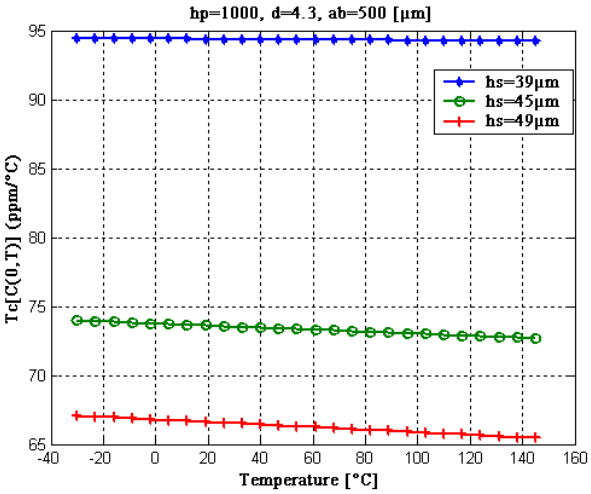

Fig. 6. Temperature Coefficient for Different Values of hs.

3.2.2. Effect of the distance between the two plates *d*

Figures 7 and 8, respectively, give the evolution of the thermal capacitance and of the temperature coefficients. The results show that the sensors with small distance

between the two plates have high thermal coefficients.

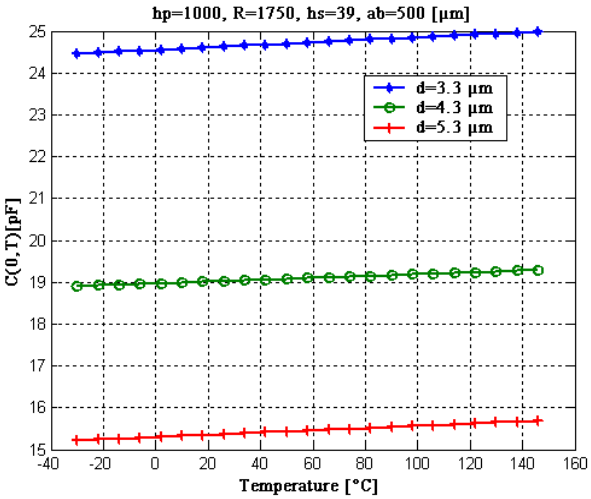

Fig. 7. Capacitance thermal variations for the different distance inter-elctrode.

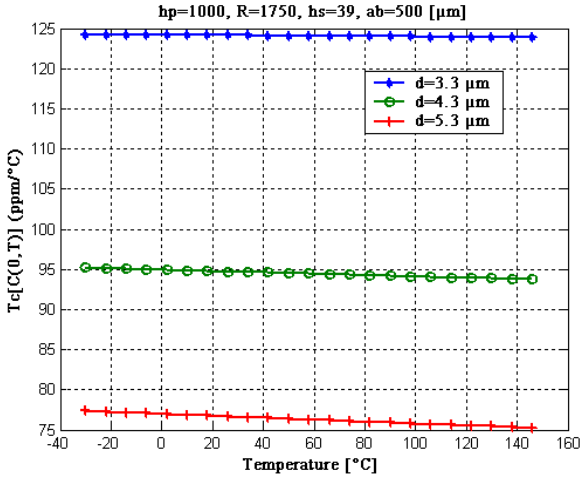

Fig. 8. Temperature Coefficient for Different Values of *d*.

3.2.3. Bonded area effect *ab*

In Fig. 9 we varied *ab* with the fixing of the other geometrical parameters; we have observed that the sensitivity to temperature impoverished by the augmentation of the bond width *ab*. Thus, whatever, the characteristics of the sensors over the welded area are large and the sensors are less sensitive to temperature. But this leads to the enlargement of the size of the device, which is a drawback.

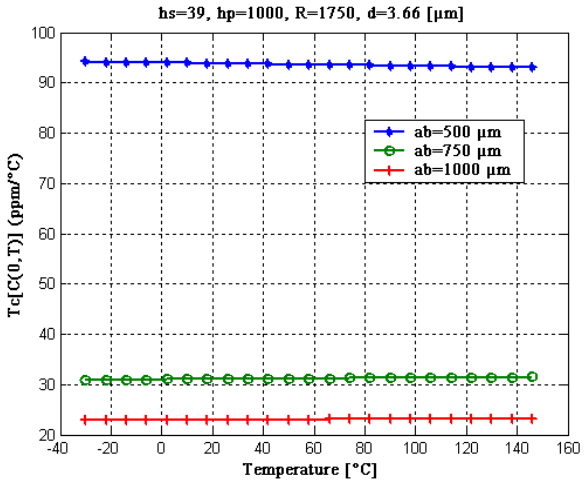

Fig. 9. Temperature coefficient for different values of *ab*.

3.3. Study based on pressure

3.3.1. Effect of the shape of the recessed membrane

We analyze the sensor response as a function of applied pressure at ambient temperature. In order to save time, it is necessary to apply all simplifications that are possible without losing accuracy. One such a simplification is offered by the symmetry. As we can see in Fig. 10, the pressure sensor may be modeled just in one quarter because the other three quarters are symmetrical.

It is clear that the deflection is proportional to the applied pressure and its value is higher in the center. So as to determine the effect of the membrane embedding shape on the deflection, the pressure sensitivity, and consequently *C*, we have studied three devices with the same membrane shapes and measurements but different by their embedding shape as it is shown from Fig. 10. From these plots we may conclude that the effect of the embedding shape is very significant.

Figure 11 shows the variations of the sensitivity as a function of the applied pressure. As we can notice, the sensitivity of the circular sensor is higher so it is better than other forms. This is the effect of the corner presented by the other two forms. For the circular shape, it has an equal sensitivity throughout its perimeter. In the contrary, concerning the other forms, the effect of the corner creates a decrease of sensitivity. Typical values of the sensitivity are summarized in the Table 2.

Table 2. Value of the maximal deflection and the sensitivity for several ship shape.

Shape	Circular	Square	Rectangular
Maximal deflection *w(r =0)* (µm)	4.215	3.7912	2. 6056
Sensitivity *S* (pF/ kPa)	0.127 0.121 [23]	0.058 >0.0285 [24]	0.022

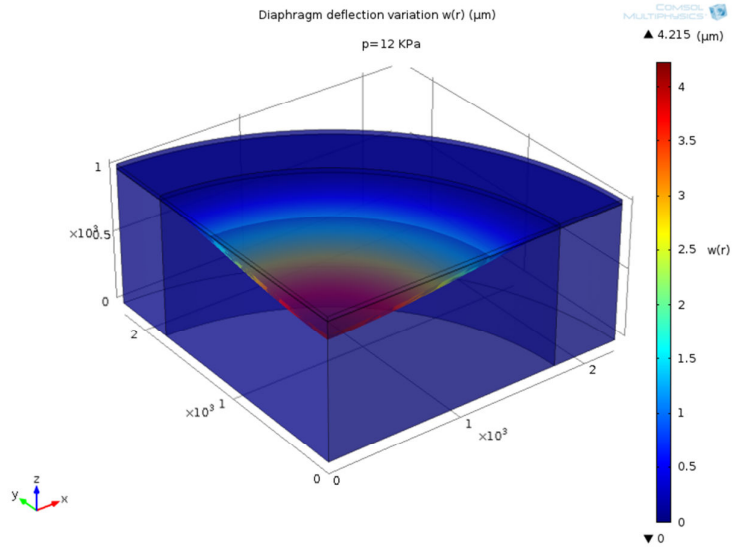

(a) Circular Chip.

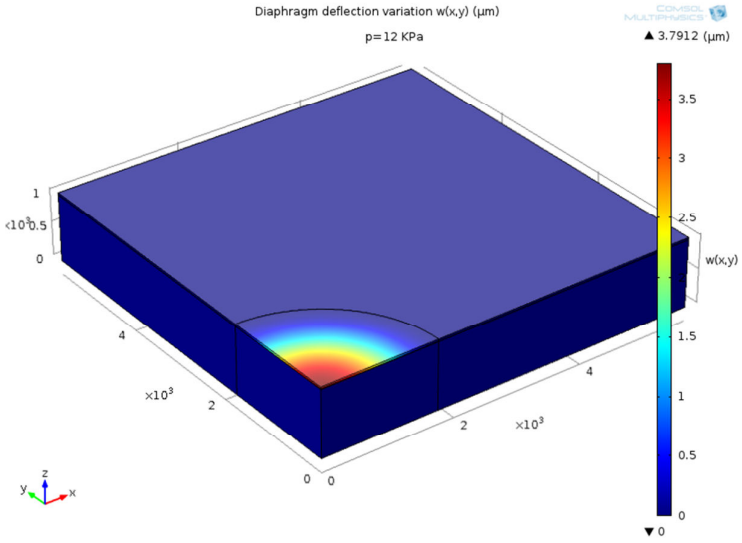

(b) Square Chip.

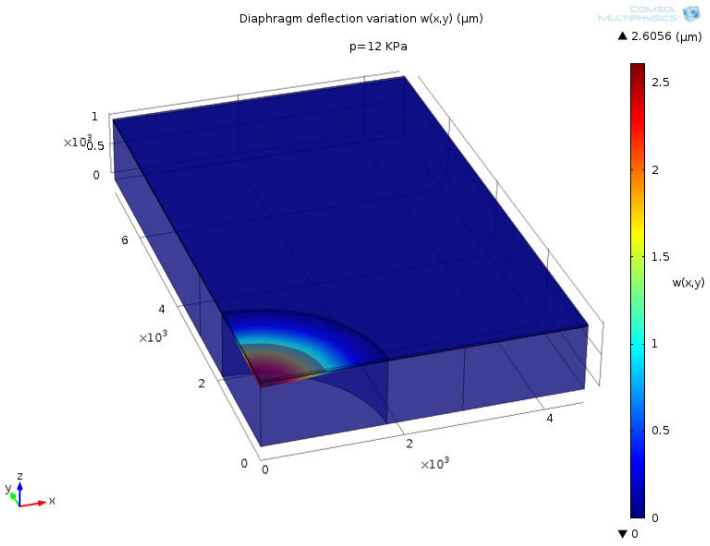

(c) Rectangular Chip.

Fig. 10. Simulation of the deflection in pressure sensor for several Membrane shapes.

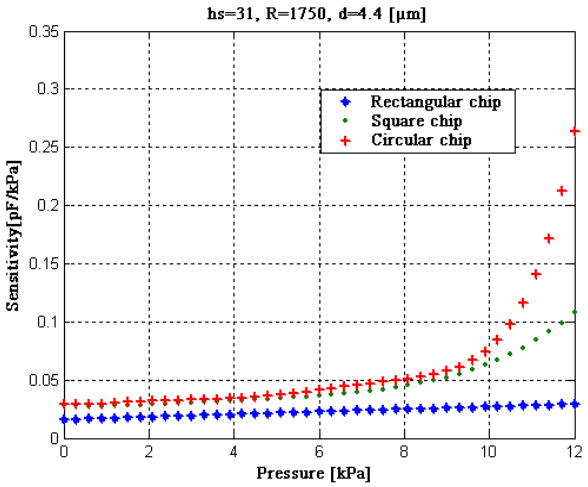

Fig.11. Capacitance sensitivity variation vs. applied pressure for several membrane shapes.

3.3.2. Effect of the membrane thickness *hs*

To highlight the effect of the thickness of the silicon membrane, we have shown in Figs. 12 and 13 the capacitance variation and the sensitivity according to the

applied pressure for several values the thickness *hs*. The *C(p)* and *S(p)* are decreasing functions of membrane thickness. Nevertheless, these variations exhibit a non-linear response.

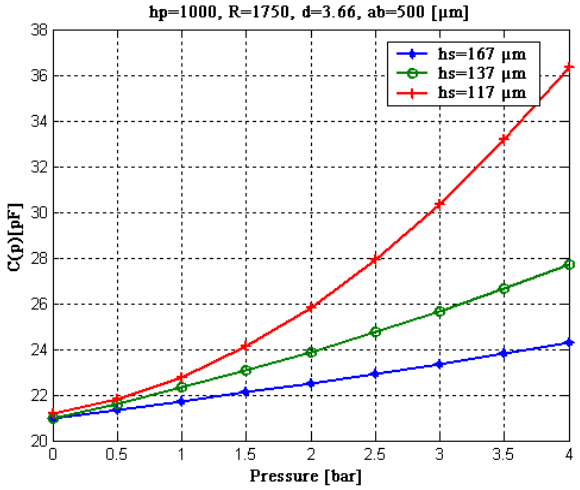

Fig. 12. Capacitance variation vs. applied pressure for several *hs*.

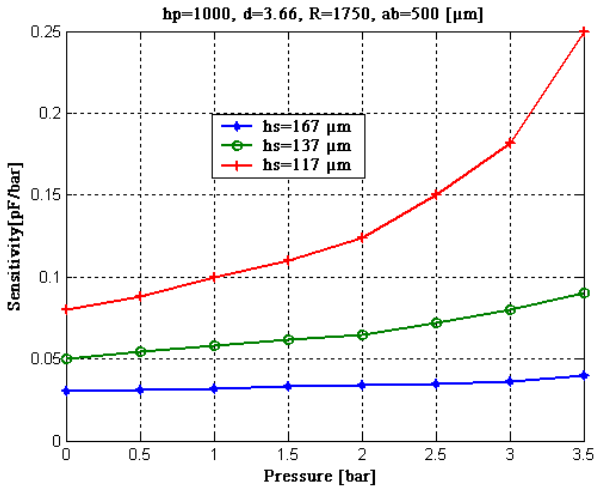

Fig. 13. Sensitivity variation vs. applied pressure *P*.

3.3.3. Effect of the dielectric thickness *d*

The capacitive response and the pressure sensitivity are inversely proportional to the distance between electrodes (Figs. 14 and 15). In order to design capacitive pressure sensors with high sensitivity to pressure, it is necessary to have a thin membrane cavity.

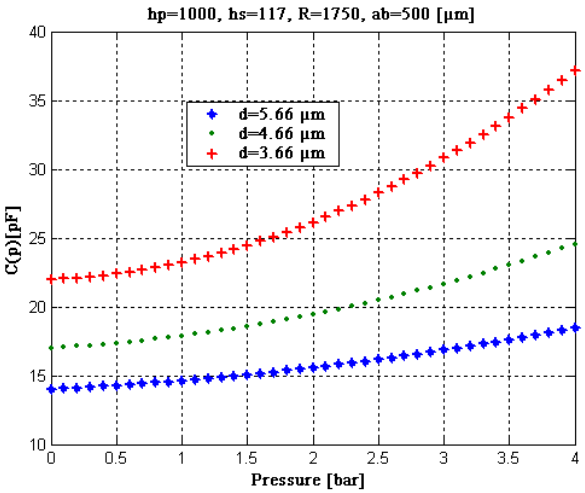

Fig. 14. Variation of capacitance vs. pressure for the different distances inter-elctrode.

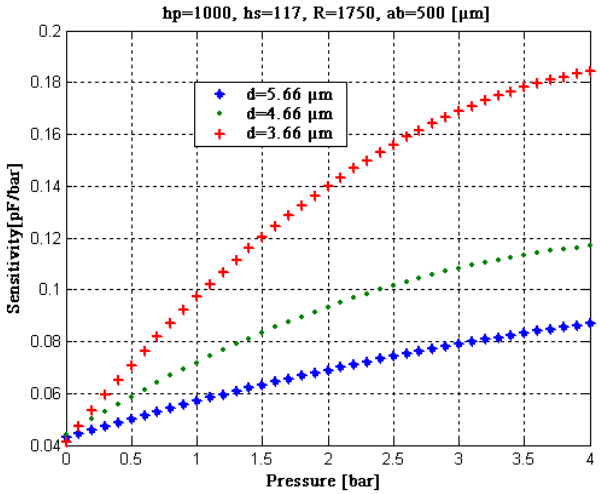

Fig. 15. Variation of sensitivity vs. pressure for the different distances inter-elctrode.

4. Conclusion

In conclusion, this paper has demonstrated that it is possible to model, with good precision, the thermal behavior of the capacitive pressure sensor using Finite Element Analysis (*FEA*) made in COMSOL.

- The choice of the modeling proposed is based on COMSOL and Matlab results studied previously [18, 25].
- The model solved in the COMSOL environment takes into consideration the integrity of the sensor. The thermal constraint due to the fabrication process has also been taken into account. This allows us to better understand and quantify the thermal drift which may undergo the sensor.
- The model developed in COMSOL also gives an opportunity to study the thermal drift of sensor characteristics at rest and under constant and uniform pressure. In addition, we attempted to study the geometric influence parameters on these characteristics to optimize the sensor performance.
- The results confirmed that the temperature coefficient is a decreasing function of the bond width, the substrate thickness and the distance between the two plates. So, to reduce thermal sensitivity, it is necessary to have a large recessed width. This solution is easy to implement and does not affect the pressure sensitivity. However, it gives large size defects.
- On the other hand, as we have pointed out earlier, for designing capacitive pressure sensors with high sensitivity to pressure, it is necessary to have a large surface and a thin membrane cavity. Nevertheless, these two parameters are themselves limited by other technological factors of manufacture such as: the dimensions of the device, the precision and reliability.
- Finally, this study allows us to optimize the sensor performance in function to the application for which it is dedicated.

Acknowledgements

The authors thank Mr Zeraoulia Hakim and Mr. Beddiaf Abdelghafour for their invaluable help for this project, which was fully done at the Constantine1 University, Faculty of Engineering Sciences, Electronics' Department, MoDERNa Laboratory. We also thank all the staff members of MoDERNa Laboratory, University Constantine1

References

1. Fatimah, Siti Abdul Rahman.; Mohammad Ismail.; Norhazilan Md.; and Noor, Hazri Bakhtiar. (2012). Embedded capacitor sensor for monitoring corrosion of reinforcement in concrete. *Journal of Engineering Science and Technology* (*JESTEC*), 7(2), 209-218.
2. Meng-Hui, Chen.; and Michael, S.C.Lu. (2008). Design and characterization of an air-coupled capacitive ultrasonic sensor fabricated in a CMOS process. *Journal of Micromechanics and Microengineering*, 18(1), 6 pages.
3. Pedersen, T.; Fragiacomo, G.; Hansen, O.; and Thomsen, E.V. (2009). Highly sensitive micromachined capacitive pressure sensor with reduced hysteresis and low parasitic capacitance. *Sensors and Actuator A: Physical,* 154(1), 35-41.
4. Lee, Y.S.; and Wise, K.D. (1982). A batch-fabricated silicon capacitive pressure transducer with low temperature sensitivity. *IEEE Trans. Electron Devices,* 29(19), 42-48.
5. Kai, Li.; Wenyuan, Chen.; and Weiping, Zhang. (2012). Design, modeling and analysis of highly reliable capacitive micro accelerometer based on

circular stepped-plate and small-area touch mode. *Microelectronics Reliability,* 52(7), 1373-1381.

6. Neumann, J.J.; Greveand, D.W.; and Oppenheim, I.J. (2004). Comparison of Piezoresistive and Capacitive Ultrasonic Transducers. *Proceedings of the Smart structures and materials Conference*, *SPIE* 5391.
7. Chavan, A.; and Wise, K.D. (1997). A batch-processed vacuum-sealed capacitive pressure sensor. *Proceedings of the 9th International Conference on Solid-State Sensors and Actuators,* 1449-1452.
8. Takahata, K.; and Gianchandani, Y.B. (2008). A Micromachined Capacitive Pressure Sensor Using a Cavity-Less Structure with Bulk-Metal/Elastomer Layers and Its Wireless Telemetry Application. *Sensors,* 8(4), 2317-2330.
9. Heung, S.L.; Chongdu, C.; and Sung, P.C. (2009). Robust designed capacitive gas pressure sensor for harsh environment. *Sensors Conference,* 770-773.
10. Shahiri, M.; Tabarestani, B.; and Ganji, A. (2012). Design and Simulation of High Sensitive Capacitive Pressure Sensor with Slotted Diaphragm. *International Conference on Biomedical Engineering,* 484-489.
11. Albahri, M. (2005). *Influence de la température sur le comportement statique et dynamique des capteurs de pression capacitifs au silicium*. Ph.D. Thesis. University of Toulouse, France.
12. Zhang, Y.; Howver, R.; Gogoi, B. ; and Yazdi, N. (2011). A high sensitivity ulta- thin MEMS capacitive pressure sensor. *IEEE International Conference on Solid-State Sensors,* 112-115.
13. Blasquez, G.; Chauffleur, X.; Pons, P.; Douziech, C.; Favaro, P.; and Menini, Ph. (2000). Intrinsic thermal behavior of capacitive pressure sensors: mechanisms and minimization. *Sensors and Actuators*, 85(1-3), 65-69.
14. Ettouhami, A.; Zahid, N.; and Elbelkacemi, M. (2004). A novel capacitive pressure structure with high sensitivity and quasi linear response. *Comptes rendus mécanique,* 332, 141-146.
15. Aljancic, U.; Resnik, D.; Vrtacnik, D.; Mozek, M.; and Amon, S. (2002). Temperature effects modeling in silicon piezoresistive pressure sensor. *Electrotechnical conference*, 36-40.
16. Boukabache, A.; Blasquez, G.; Pons P.; and Dibi, Z. (1999). Study of the thermal drift of the offset voltage of silicon pressure sensor. *IEEE International Conference on Electronics, Circuits and Systems,* 1051-1054.
17. Abdelaziz, Beddiaf., Fouad, Kerrour., and Salah Kemouche. (2014). The Effect of Temperature and Doping Level on the Characteristics of Piezoresistive Pressure Sensor. *Journal of Sensor Technology*, 4, 59-65.
18. Abdelaziz, Beddiaf., Fouad, Kerrour., and Salah Kemouche. (2014). Thermo mechanical Modeling of Piezoresistive Pressure Sensor. *International Review on Modelling and Simulations (I.RE.MO.S.),* 7(3), 517-522.
19. Catling, D.C. (1998). High sensitivity capacitive sensors for measuring medium-vacuum gas pressure. *Sensors and actuator A* 64(2), 157-164.
20. Timochenko, S.P.; and Woinoiwsky-Krieger, S. (1982). *Theory of plates and shells.* McGraw-Hill.

21. Wortmans, J.J.; and Evans, R.A. (1965). Young's modulus, Shear modulus and Poisson's ratio in Silicon and Germanium. *Journal of Applied Physics,* 36(1), 153.
22. Chauffleur, X. (1998). *Modélisation par la méthode des éléments finis du comportement thermomécanique de capteurs de pression capacitifs et piézorésistifs en silicium*. Ph.D. Thesis. University of Toulouse, France.
23. Bao, M.H. (2000). *Micro Mechanical Transducers Pressure Sensors, Accelerometers and Gyroscopes*. Handbook of sensors and actuators.
24. Menini, P. (1998). *Faisabilité d'un capteur de pression capacitif miniature sur silicium*. Ph.D. Thesis. University of Toulouse, France.
25. Fouad, Kerrour., and Farida, Houbar. (2006). A novel numerical approach for the modeling of the square shaped silicon membrane. *Semiconductor Physics, Quantum Electronics & Optoelectronics,* 7(3), 52-57.